NAVY DEPARTMENT

THE DAVID W. TAYLOR MODEL BASIN

WASHINGTON 7, D.C.

SUPER-CAVITATING FLOW PAST BODIES WITH FINITE LEADING EDGE THICKNESS

by

J. N. Newman

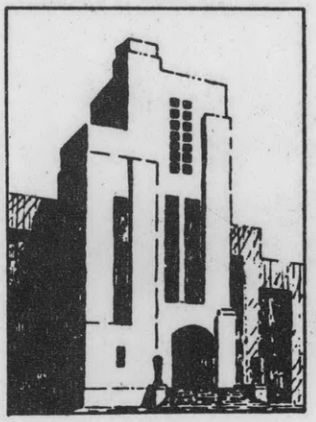

RESEARCH AND DEVELOPMENT REPORT

1

SEPTEMBER 1956 Report 1081

SUPER-CAVITATING FLOW PAST BODIES WITH FINITE LEADING EDGE THICKNESS

by

J. N. Newman

SEPTEMBER 1956 Report 1081

TABLE OF CONTENTS

SUMMARY

STATEMENT OF THE PROBLEM

The problem to be considered is the effect of increasing the leading edge thickness of a supercavitating foil beyond the cavity thickness, such that a portion of the back near the leading edge becomes wetted and cavitation does not commence until some point downstream from the leading edge.

FINDINGS

The investigation has resulted in an approximate solution for the lift and drag on a foil with a finite leading edge. The solution shows that there is a very large decrease in the lift-drag ratio due to the wetted portion of the back, and as such it seems advisable whenever possible to avoid using a foil with a thick leading edge. It was not determined however, at what angle of attack this type of flow would occur for a given foil with some arbitrary leading edge thickness.

RECOMMENDATIONS

It is recommended that the above-mentioned type of flow be avoided by keeping the thickness of the leading edge less than the cavity thickness. It is also suggested that further research be devoted to determining the critical angle of attack at which the back will be partially wetted, and to determine an exact solution by a conformal mapping technique.

NOTATION

b	A constant, undefined in terms of physical parameters
C_D	Drag coefficient = $\frac{D}{\frac{1}{2}\rho s U_\infty^2}$
C_L	Lift Coefficient = $\frac{L}{\frac{1}{2}\rho s U_\infty^2}$
D	Drag
D_1	Drag component due to the back
D_2	Drag component due to the face
L	Lift
L_1	Lift component due to the back
L_2	Lift component due to the face
ℓ	Cavity length measured from the leading edge
m	Strength of a source distribution
p	Local static pressure
P_c	Cavity pressure
P_o	Pressure on the body
P_∞	Static pressure of the stream at infinity
R	Radius of the arc of the Circular Arc Section
Re	Denotes "the real part of"
r	Ratio of upper to lower chord lengths: $r = \frac{S_1}{S_2}$
s	Chord length
s_1	Chord length of the back (upper surface) measured to the point of cavitation inception
s_2	Chord length of the face (lower surface)
t	Dummy variable
U_c	The x-component of the velocity on the cavity wall
U_∞	The stream velocity at infinity

u	The x-component of the perturbation velocity
u_{c-o}	The x-component of the perturbation velocity which is induced by the cavity source distribution
u_{o-o}	The x-component of the perturbation velocity which is induced by the body source distribution
$\vec{V}$	The velocity of the fluid at any point in the flow field
$\vec{v}$	The local perturbation velocity, $\vec{v} = \vec{V} - U_\infty$
v	The y-component of the perturbation velocity
v_c	The y-component of the perturbation velocity on the cavity
v_o	The y-component of the perturbation velocity on the body
x	A space coordinate parallel to U_∞
x'	A dummy variable
Y	A space coordinate, orthogonal to the x-direction
Y_o	Y-ordinate of the foil surface
Y_1	Y-ordinate of the back
Y_2	Y-ordinate of the face
Z	A dummy variable
α_1	The slope of the back when it is constant (up to s_1)
α_2	The slope of the face when it is constant
ρ	Fluid density
σ	Cavitation number, $\sigma = \frac{P_\infty - P_o}{\frac{1}{2}\rho U_\infty^2}$
τ	A dummy variable
ϕ	Velocity potential
χ	A dummy variable
ω	A constant defined by $\omega = \frac{\pi\alpha_1}{\alpha_1 + \alpha_2}$

ABSTRACT

An approximate method is developed for determining the coefficients of lift and drag for a foil whose face is completely wetted and whose back is wetted up to a certain point and cavitating downstream of that point, at zero cavitation number. The solution obtained is compared with exact theory for flow past a flat plate, with exact theory for flow past a non-symmetrical wedge, and with available experimental results.

INTRODUCTION

The effects of cavitating flow past flat plates and thin foils have been the subject of recent research by Tulin[1] and Wu[2]. Both developed linearized theories for the flow and solved the problems by conformal mapping. In this way they determined the lift and drag of the cavitating hydrofoil as a function of the drag and moment of the equivalent airfoil.

The limitation that the thickness of such a foil be less than the cavity thickness presents practical difficulties near the leading edge where the cavity approaches zero thickness and leads to vibration and buckling of the foil. It was, therefore, considered desirable to investigate the effects of increasing the leading edge thickness to some value greater than the cavity thickness. For such a section the theory based on thin foils will not hold since the back is no longer fully cavitating. Consequently, an attempt has been made to solve the problem using potential flow theory in a manner similar to that used by Tulin to investigate the flow past a symmetrical wedge[3].

THEORY

Two methods have been used to develop approximate solutions for cavitating flow. The most popular is the determination of a mathematical model for an equivalent flow. Birkhoff[4] and Gilbarg and Rock[5] give accounts of early work along these lines to determine the flow past flat plates perpendicular to the stream. More recently Tulin and Wu developed linearized solutions for flow past thin lifting surfaces. The other method is the application of linearized potential flow theory to determine a source distribution and from this to determine the velocity and pressure distribution on the surface of the body. This is the method used by Tulin[3] to determine the cavity shape and drag of a symmetrical wedge.

The equivalent airfoil was not used in the present problem because of the additional singularity at the leading edge which is not present in the thin foil problem. Consequently, linearized potential flow theory was used in a manner similar to that of Tulin[3].

---

[1]References are listed on Page 18

The presence of a finite leading edge thickness prevents the inception of back cavitation at the leading edge. Back cavitation does not commence until some point s_1 and continues from there to the extremity of the cavity at some point ℓ. For sufficiently low cavitation numbers the cavity length will be large relative to the lower chord length, a condition necessary for the development of the theory.

It is assumed that no cavitation occurs on the pressure side until the termination of the chord length, s_2, and the cavity extends out to ℓ (Figure 1). It is also assumed that the slopes of the upper and lower faces, $\frac{dy_1}{dx}$ and $\frac{dy_2}{dx}$ respectively, and the chord lengths s_1 and s_2 are such that no cavitation occurs on either the face or the back in the intervals $0 \leqq x \leqq s_1$ and $0 \leqq x \leqq s_2$. For this to be true the stagnation point must be at the leading edge.

The problem then resolves to that of finding a source distribution which will produce this flow, and to determine from it the pressure distribution along the wetted portions of the face and back. The pressure on the back beyond the point s_1 (i.e. the portion of the back lying inside the cavity) is assumed to be at the cavity pressure. Consequently, the pressure at any point on the surface of the foil will be known and by suitable integration the lift and drag can be determined.

SOURCE DISTRIBUTION SOLUTION

BOUNDARY CONDITIONS

On the wetted portions of the face and back the streamline slope is equal to the slope of the body:

$$\frac{dy_1}{dx}(x) = \frac{v(x,y_1)}{U_\infty + u(x,y_1)} = \frac{v(x,y_1)}{U_c}\left[1 - \frac{u(x,y_1)-u(x,y_{c1})}{U_c} + O\left(\frac{u(x,y_1)-u(x,y_{c1})}{U_c}\right)^2\right] \qquad (1)$$

$$\frac{dy_2}{dx}(x) = \frac{v(x,y_2)}{U_\infty + u(x,y_2)} = \frac{v(x,y_2)}{U_c}\left[1 - \frac{u(x,y_2)-u(x,y_{c2})}{U_c} + O\left(\frac{u(x,y_2)-u(x,y_{c2})}{U_c}\right)^2\right] \qquad (2)$$

On the cavity wall the pressure is p_c and using Bernoulli's equation this determines the cavitation number as a function of the cavity wall velocity and the stream velocity:

$$\sigma = \frac{2u(x,y_c)}{U_\infty} + O\left(\frac{v(x,y_c)}{U_\infty}\right)^2 = 2\left(\frac{U_c}{U_\infty} - 1\right) + O\left(\frac{v(x,y_c)}{U_\infty}\right)^2 \qquad (3)$$

where Equation (3) holds over both surfaces.

When linearized, these three equations give:

$$\frac{dy_1}{dx}(x) = \frac{v(x,0+)}{U_c} \qquad 0 < x < s_1 \qquad (1a)$$

$$\frac{dy_2}{dx}(x) = \frac{v(x,0-)}{U_c} \qquad 0 < x < s_2 \qquad (2a)$$

$$\sigma = \frac{2u(x,0+)}{U_\infty} \qquad s_1 < x < \ell \qquad (3a)$$

$$\sigma = \frac{2u(x,0-)}{U_\infty} \qquad s_2 < x < \ell \qquad (3b)$$

The remaining boundary condition is that at the two points where cavitation commences the flow must be smooth. Consequently, the slope of the cavity must be continuous with the slope of the body. This condition is satisfied by eliminating solutions for the source distribution which go to infinity at these points.

SOLUTION

The following solution is based on the simplified assumption that, with the stagnation point at the leading edge, the flow on the face is independent of the geometry of the back. Consequently, the flow on each surface is assumed to be the same as that on a symmetrical body of the same slope and chord length as the surface in question. The lift is then assumed to be the difference between the lifts of the two surfaces considered separately, and the drag is assumed to be the sum of the two drags. This is a crude assumption since it assumes that the stagnation streamline will be horizontal as it approaches the leading edge, and this will not be the case unless the foil is symmetrical, in which case of course there will be no lift. However, this procedure should give an approximate solution and was followed.

Since the two surfaces can be treated separately, the development is based on a single surface of slope dy_o/dx and chord length s, and which may be applied to either the face or the back.

A distribution of sources of strength m(x) along the x-axis in the interval $0<x<\ell$ gives the following:

$$\phi(x,y) = \int_0^\ell \frac{m(x') \ln w \, dx'}{2\pi} \qquad \text{where} \quad w = \sqrt{(x-x')^2 + y^2} \tag{4}$$

and thus:

$$u(x,y) = \frac{\partial \phi}{\partial x} = \frac{1}{2\pi}\int_0^\ell \frac{m(x')(x-x')\,dx'}{w^2} \tag{5}$$

$$v(x,y) = \frac{\partial \phi}{\partial y} = \frac{1}{2\pi}\int_0^\ell \frac{m(x')y\,dx'}{w^2} \tag{6}$$

At points on the x-axis the perturbation velocities u(x,0) and v(x,0) will be:

$$u(x,0) = \frac{1}{2\pi}\int_0^\ell \frac{m(x')\,dx'}{x-x'} \tag{7}$$

$$v(x,0) = \frac{1}{2} m(x) \tag{8}$$

The boundary conditions on the x-axis will be satisfied if:

$$m(x) = 2U_c \frac{dy_o}{dx} \qquad 0<x<s \tag{9}$$

and thus

$$\frac{1}{2\pi}\int_0^s \frac{2U_c \frac{dy_o}{dx'}(x')\,dx'}{x-x'} + \frac{1}{2\pi}\int_s^\ell \frac{m(x')\,dx'}{x-x'} = \frac{U_\infty \sigma}{2} \qquad s<x<\ell \tag{10}$$

The problem may then be formulated: to find m(x) such that:

$$\int_s^\ell \frac{m(x')dx'}{x-x'} = \pi\sigma U_\infty - 2U_c \int_0^s \frac{\frac{dy_o}{dx'}\,dx'}{x-x'} = f(x) \tag{11}$$

and

$$\int_s^\ell m(x')\,dx' = -\int_0^s 2U_c \frac{dy_o}{dx'}\,dx' = -2U_c\, y(s) \tag{12}$$

Using the thin airfoil theory inversion formula[6] gives m(x) from Equation (11):

$$m(x) = \frac{1}{\pi\sqrt{(x-s)(\ell-x)}} \int_s^\ell \frac{\sqrt{(x'-s)(\ell-x')}}{(x'-x)} \left(\frac{1}{\pi} f(x')\right) dx' + b$$

$$m(x) = \frac{1}{\pi^2\sqrt{(x-s)(\ell-x)}} \left\{ \int_s^\ell \frac{\sqrt{(x'-s)(\ell-x')}}{(x'-x)} \left[\pi\sigma U_\infty - 2U_c \int_0^s \frac{\frac{dy_0}{dt}\, dt}{(x'-t)}\right] dx' + b \right\}$$

To satisfy the juncture condition the term in brackets must vanish at x=s:

$$0 = b + \pi\sigma U_\infty \int_s^\ell \frac{\sqrt{(x'-s)(\ell-x')}\, dx'}{(x'-s)} - 2U_c \int_s^\ell \frac{\sqrt{(x'-s)(\ell-x')}}{(x'-s)} \int_0^s \frac{\frac{dy_0}{dt}\, dt}{(x'-t)} dx'$$

$$b = -\int_s^\ell \sqrt{\frac{\ell-x'}{x'-s}} \left[\pi\sigma U_\infty - 2U_c \int_0^s \frac{dy_0}{dt} \frac{dt}{x'-t}\right] dx'$$

therefore:

$$m(x) = \frac{1}{\pi^2}\sqrt{\frac{x-s}{\ell-x}} \int_s^\ell \sqrt{\frac{\ell-x'}{x'-s}} \frac{1}{(x'-x)} \left[\pi\sigma U_\infty - 2U_c \int_0^s \frac{dy_0}{dt} \frac{dt}{(x'-t)}\right] dx' \qquad (13)$$

Evaluating the integrals as shown in Appendix A gives:

$$m(x) = -\sigma U_\infty \sqrt{\frac{x-s}{\ell-x}} + \frac{2U_c}{\pi}\sqrt{\frac{x-s}{\ell-x}} \int_0^s \frac{dy_0}{dt} \sqrt{\frac{t-\ell}{t-s}} \frac{dt}{(x-t)} \qquad (13a)$$

For the case of zero cavitation number, $\sigma = 0$, $U_c = U_\infty$, and $\ell \to \infty$:

$$m(x)_{\sigma=0} = \frac{2U_\infty}{\pi}\sqrt{x-s} \int_0^s \frac{dy_0}{dt} \frac{dt}{(x-t)\sqrt{s-t}} \qquad (13b)$$

DETERMINATION OF LIFT AND DRAG

DRAG

Assuming the foil to be deeply submerged in an ideal flow (i.e., neglecting frictional and wave resistance) the drag on one surface will be given by the integral:

$$D = \int_0^S (p_o - p_c)\frac{dy_o}{dt}\,dt = \rho\left[U_c^2 + v_c^2\right]\int_0^S \left[1 - \frac{U_o^2 + v_o^2}{U_c^2}\right]\frac{dy_o}{dt}\,dt \tag{14}$$

which may also be written:

$$D = \rho\left[U_c^2 + v_c^2\right]\int_0^S \left[-\left(\frac{U_o - U_c}{U_c}\right) - \left(\frac{U_o - U_c}{U_c}\right)^2 - \frac{V_o^2}{U_c^2}\right]\frac{dy_o}{dt}\,dt \tag{14a}$$

and after linearization this becomes:

$$D = -\rho U_c \int_0^S \left[u(t, y_o) - u(t, y_c)\right]\frac{dy_o}{dt}\,dt \tag{14b}$$

but $u(t,y_o) = u_{o-o}(t,y_o) + u_{c-o}(t,y_o)$

where $u_{o-o}(t,y_o)$ is the x component of that part of the disturbance velocity on the body which is induced by the cavity source distribution and $u_{c-o}(t,y_o)$ is the x component of that part of the disturbance velocity on the body which is induced by the cavity source distribution.

since: $$\int_0^S u_{o-o}(t, y_o)\frac{dy_o}{dt}\,dt = 0$$

and $$u(t, y_c) = \tfrac{1}{2}\sigma U_\infty$$

the equation for drag becomes:

$$D = \rho U_c \left\{ \frac{1}{2} \sigma U_\infty y_o(s) - \int_o^s u_{c-o}(t, y_o) \frac{dy_o}{dt} dt \right\} \tag{14c}$$

The integral term in (14c) is evaluated as follows:

using equations (7) and (13a):

$$\int_o^s u_{c-o}(t, y_o) \frac{dy_o}{dt} dt = \int_o^s \frac{1}{2\pi} \frac{dy_o}{dt} \int_s^\ell \frac{m(x')\,dx'}{t-x'} dt$$

$$= \frac{1}{2\pi} \int_o^s \frac{dy}{dt} \int_s^\ell \frac{1}{t-x'} \left[-\sigma U_\infty \sqrt{\frac{x'-s}{\ell-x'}} + \frac{2U_c}{\pi} \sqrt{\frac{x'-s}{\ell-x'}} \int_o^s \frac{dy_o}{d\tau} \sqrt{\frac{\tau-\ell}{\tau-s}} \frac{d\tau}{x'-\tau} \right] dx'dt$$

$$= \frac{\sigma U_\infty}{2\pi} \int_o^s \frac{dy_o}{dt} \int_s^\ell \sqrt{\frac{x'-s}{\ell-x'}} \frac{1}{t-x'} dx'dt + \frac{U_c}{\pi^2} \int_o^s \frac{dy_o}{dt} \int_s^\ell \sqrt{\frac{x'-s}{\ell-x'}} \frac{1}{(t-x')} \int_o^s \frac{dy_o}{d\tau} \sqrt{\frac{\tau-\ell}{\tau-s}} \frac{dt}{x'-\tau} dx'dt \tag{15}$$

Using Appendix A the first term of Equation (15) is evaluated:

$$-\frac{\sigma U_\infty}{2\pi} \int_o^s \frac{dy_o}{dt} \int_s^\ell \sqrt{\frac{x'-s}{\ell-x'}} \frac{dx'}{t-x'} dt = \frac{-\sigma U_\infty}{2} \int_o^s \frac{dy_o}{dt} \sqrt{\frac{t-s}{t-\ell}}\, dt + \frac{\sigma U_\infty}{2} y_o(s)$$

And using Appendix B the second term of Equation (15) is:

$$\frac{U_c}{2\pi} (s-\ell) \left[\int_o^s \frac{dy_o}{dt} \frac{dt}{\sqrt{(t-s)(t-\ell)}} \right]^2$$

therefore:

$$\int_o^s u_{c-o}(t,y_o)\frac{dy_o}{dt}\,dt = -\frac{\sigma U_\infty}{2}\int_o^s \frac{dy_o}{dt}\sqrt{\frac{t-s}{t-\ell}}\,dt + \frac{\sigma U_\infty}{2}\,y_o(s)$$

$$+\frac{U_c}{2\pi}(s-\ell)\left[\int_o^s \frac{dy_o}{dt}\frac{dt}{\sqrt{(t-s)(t-\ell)}}\right]^2 \qquad (15a)$$

And Equation (14c) becomes:

$$D = \tfrac{1}{2}\rho U_c U_\infty \int_o^s \frac{dy_o}{dt}\sqrt{\frac{t-s}{t-\ell}}\,dt - \frac{\rho U_c^2}{2\pi}(s-\ell)\left[\int_o^s \frac{dy_o}{dt}\frac{dt}{\sqrt{(t-s)(t-\ell)}}\right]^2 \qquad (14d)$$

the drag coefficient, $C_D = \dfrac{D}{1/2\,\rho U_\infty^2 s}$, is then obtained, remembering that, from Equation (3), $U_c = U_\infty(1 + 1/2\,\sigma)$:

$$C_D = \frac{\sigma(1+\frac{1}{2}\sigma)}{s}\int_o^s \frac{dy_o}{dt}\sqrt{\frac{t-s}{t-\ell}}\,dt - \frac{(1+\frac{1}{2}\sigma)^2}{\pi s}(s-\ell)\left[\int_o^s \frac{dy_o}{dt}\frac{dt}{\sqrt{(t-s)(t-\ell)}}\right]^2 \qquad (16)$$

LIFT

The lift is calculated in the same manner as was the drag. Assuming small angles of attack, the lift of one surface will be:

$$L = \int_o^s (p_o - p_c)\,dt \qquad (17)$$

In Equation (17) and hereafter, the following convention is used: in a flow from left to right (Figure 1) lift up is positive; slope up and to the right is negative, and slope down and to the right is positive, corresponding to the usual angle of attack.

Linearizing as in Equation (14) gives:

$$L = -\rho U_c \int_0^S \left[u(t,y_0) - u(t,y_c) \right] dt \tag{17a}$$

and $u(t,y_0) = u_{o-o}(t,y_0) + u_{c-o}(t,y_0)$

The integration that follows is considerably simplified by making the second assumption; namely, that:

$$\int_0^S u_{o-o}(t,y_0)\, dt = 0$$

Equation (17a) thus becomes:

$$L = \rho U_c \left\{ \tfrac{1}{2}\sigma U_\infty S - \int_0^S u_{c-o}(t,y_0)\, dt \right\} \tag{17b}$$

and proceeding as for drag:

$$\int_0^S u_{c-o}(t,y_0)\, dt = \int_0^S \frac{1}{2\pi} \int_S^\ell \frac{m(x')\,dx'}{t-x'}\, dt$$

$$= \frac{1}{2\pi} \int_0^S \int_S^\ell \frac{1}{t-x'} \left[-\sigma U_\infty \sqrt{\frac{x'-S}{\ell-x'}} + 2\frac{U_c}{\pi} \sqrt{\frac{x'-S}{\ell-x'}} \int_0^S \frac{dy_0}{d\tau} \sqrt{\frac{\tau-\ell}{\tau-S}}\, \frac{d\tau}{x'-\tau} \right] dx'\, dt$$

$$= -\frac{\sigma U_\infty}{2\pi} \int_0^S \int_S^\ell \sqrt{\frac{x'-S}{\ell-x'}}\, \frac{dx'}{t-x'}\, dt + \frac{U_c}{\pi^2} \int_0^S \int_S^\ell \sqrt{\frac{x'-S}{\ell-x'}}\, \frac{1}{t-x'} \int_0^S \frac{dy_0}{d\tau} \sqrt{\frac{\tau-\ell}{\tau-S}}\, \frac{d\tau}{x'-\tau}\, dx'\, dt \tag{18}$$

The first term of Equation (18) is evaluated from Appendix A:

$$-\frac{\sigma U_\infty}{2\pi} \int_0^S \int_S^\ell \sqrt{\frac{x'-S}{\ell-x'}}\, \frac{dx'}{t-x'}\, dt = -\frac{\sigma U_\infty}{2} \int_0^S \sqrt{\frac{t-S}{t-\ell}}\, dt + \frac{\sigma U_\infty}{2} S$$

$$= \tfrac{1}{2}\sigma U_\infty S + \tfrac{1}{2}\sigma U_\infty \sqrt{\ell S} - \tfrac{1}{2}\sigma U_\infty (\ell - S) \ln \frac{\sqrt{\ell-S}}{\sqrt{\ell}+\sqrt{S}}$$

And the second term becomes:

$$\frac{2U_c}{\pi}\int_0^S \frac{dy}{d\tau}\left(\ln\frac{\sqrt{\ell(s-t)}+\sqrt{s(\ell-t)}}{\sqrt{(\ell-s)(s-\tau)}}\right)d\tau - \frac{2U_c}{\pi}\left(\ln\frac{\sqrt{\ell}+\sqrt{s}}{\sqrt{\ell-s}}\right)\int_0^S \frac{dy_o}{d\tau}\sqrt{\frac{\tau-\ell}{\tau-s}}\,d\tau$$

The equation for Lift is then:

$$L = \tfrac{1}{2}\rho U_c U_\infty \sigma\left[(\ell-s)\ln\frac{\sqrt{\ell-s}}{\sqrt{\ell}+\sqrt{s}} - \sqrt{\ell s}\right] + \frac{2\rho U_c^2}{\pi}\ln\frac{\sqrt{\ell}+\sqrt{s}}{\sqrt{\ell-s}}\int_0^S \frac{dy_o}{d\tau}\sqrt{\frac{\tau-\ell}{\tau-s}}\,d\tau$$

$$- \frac{2\rho U_c^2}{\pi}\int_0^S \frac{dy_o}{d\tau}\left(\ln\frac{\sqrt{\ell(s-\tau)}+\sqrt{s(\ell-\tau)}}{\sqrt{(\ell-s)(s-\tau)}}\right)d\tau \qquad (17c)$$

And:

$$C_L = \sigma(1+\tfrac{1}{2}\sigma)\left[\left(\frac{\ell}{s}-1\right)\left(\ln\frac{\sqrt{\ell-s}}{\sqrt{\ell}+\sqrt{s}}\right) - \sqrt{\frac{\ell}{s}}\right] + \frac{4}{\pi s}(1+\tfrac{1}{2}\sigma)^2\left(\ln\frac{\sqrt{\ell}+\sqrt{s}}{\sqrt{\ell-s}}\right)\int_0^S \frac{dy_o}{d\tau}\sqrt{\frac{\tau-\ell}{\tau-s}}\,d\tau$$

$$- \frac{4}{\pi s}(1+\tfrac{1}{2}\sigma)^2\int_0^S \frac{dy_o}{d\tau}\left(\ln\frac{\sqrt{\ell(s-\tau)}+\sqrt{s(\ell-\tau)}}{\sqrt{(\ell-s)(s-\tau)}}\right)d\tau \qquad (17d)$$

LIFT AND DRAG AT ZERO CAVITATION NUMBER

The expressions for lift and drag can be considerably simplified by assuming zero cavitation number. Thus the cavity length is infinite and the velocity on the cavity wall equals the stream velocity ($U_c = U_\infty$). Using Equation (13b) and proceeding as before, the expressions for lift and drag become:

$$L = -\rho U_\infty \int_0^S u_{c-o}(t, y_o)\,dt = -\frac{\rho U_\infty}{2\pi}\int_0^S\int_S^\infty \frac{2U_\infty\sqrt{x'-s}}{\pi(t-x')}\int_0^S \frac{dy_o}{d\tau}\frac{d\tau}{(x'-\tau)\sqrt{s-\tau}}\,dx'dt \qquad (18)$$

$$D = -\rho U_\infty \int_0^S u_{c-o}(t, y_o)\frac{dy_o}{dt}\,dt = \frac{-\rho U_\infty}{2\pi}\int_0^S \frac{dy_o}{dt}\int_S^\infty \frac{2U_\infty\sqrt{x'-s}}{\pi(t-x')}\int_0^S \frac{dy_o}{d\tau}\frac{d\tau}{(x'-\tau)\sqrt{s-\tau}}\,dx'dt \qquad (19)$$

and changing the order of integration,

$$L = -\frac{\rho U_\infty^2}{\pi^2}\int_0^s \frac{dy_0}{d\tau}\frac{1}{\sqrt{s-\tau}}\int_0^s\int_s^\infty \frac{\sqrt{x'-s}}{(t-x')(x'-\tau)}\,dx'\,dt\,d\tau \tag{18b}$$

$$= -\frac{\rho U_\infty^2}{\pi^2}\int_0^s \frac{dy_0}{d\tau}\frac{1}{\sqrt{s-\tau}}\int_0^s \frac{1}{t-\tau}\int_s^\infty\left(\frac{\sqrt{x'-s}}{x'-\tau}-\frac{\sqrt{x'-s}}{x'-t}\right)dx'\,dt\,d\tau$$

$$= -\frac{\rho U_\infty^2}{\pi}\int_0^s \frac{dy_0}{d\tau}\int_0^s\left(\frac{1}{t-\tau}\right)\left(\sqrt{\frac{s-t}{s-\tau}}-1\right)dt\,d\tau$$

$$= -\frac{2\rho U_\infty^2}{\pi}\left\{\int_0^s \frac{dy_0}{dt}\ln\left(1+\sqrt{\frac{s}{s-t}}\right)dt-\int_0^s\frac{dy_0}{dt}\sqrt{\frac{s}{s-t}}\,dt\right\} \tag{18c}$$

where in the last equation the variable has been changed from τ to t, to conform with the other equations.

Equation (19), likewise, becomes:

$$D=\frac{-\rho U_\infty^2}{\pi}\int_0^s\frac{dy_0}{d\tau}\int_0^s\frac{dy_0}{dt}\left(\frac{1}{t-\tau}\right)\left(\sqrt{\frac{s-t}{s-\tau}}-1\right)dt\,d\tau \tag{19b}$$

And using the procedure of Appendix B:

$$D=\frac{\rho U_\infty^2}{2\pi}\left[\int_0^s\frac{dy_0}{dt}\frac{dt}{\sqrt{s-t}}\right]^2 \tag{19c}$$

Dividing Equations (18c) and (19c) by $1/2\rho U_\infty^2 s$ gives the lift and drag coefficients:

$$C_L=-\frac{4}{\pi s}\left\{\int_0^s\frac{dy_0}{dt}\ln\left(1+\sqrt{\frac{s}{s-t}}\right)dt-\int_0^s\frac{dy_0}{dt}\sqrt{\frac{s}{s-t}}\,dt\right\} \tag{18d}$$

$$C_D=\frac{1}{\pi s}\left[\int_0^s\frac{dy_0}{dt}\frac{dt}{\sqrt{s-t}}\right]^2 \tag{19d}$$

Equation (18d) can be simplified by further linearization using the series:

$$\ln(1+z) = 2\left[\frac{z}{2+z} + \frac{1}{3}\left(\frac{z}{2+z}\right)^3 + \frac{1}{5}\left(\frac{z}{2+z}\right)^5 + \ldots\right]$$

Neglecting all but the first-power term in the series gives:

$$C_L = \frac{4}{\pi S}\int_0^S \frac{dy_0}{dt}\left[\sqrt{\frac{S}{S-t}} - \ln\left(1+\sqrt{\frac{S}{S-t}}\right)\right] \cong \frac{4}{\pi}\int_0^S \frac{dy_0}{dt}\left(\frac{dt}{2(S-t)+\sqrt{S(S-t)}}\right)dt \qquad (18e)$$

Final linearized lift and drag coefficients at zero cavitation number are then:

$$C_L = \frac{4}{\pi}\int_0^S \frac{dy_0}{dt}\frac{dt}{2(S-t)+\sqrt{S(S-t)}} \qquad (18f)$$

$$C_D = \frac{1}{\pi S}\left[\int_0^S \frac{dy_0}{dt}\frac{dt}{\sqrt{S-t}}\right]^2 \qquad (19d)$$

APPLICATION TO FOILS WITH FINITE LEADING EDGE THICKNESS AT ZERO CAVITATION NUMBER

For the case of a foil such as is shown in Figure 1, the assumption is made that the total lift and drag are the sums of the components of the lift and drag determined separately on the face and the back. Thus:

$$L = L_1 + L_2 = \frac{2\rho U_\infty^2}{\pi}\left\{\int_0^{S_1}\frac{dy_1}{dt}\left(\frac{S_1\,dt}{2(S_1-t)+\sqrt{S_1(S_1-t)}}\right) + \int_0^{S_2}\frac{dy_2}{dt}\left(\frac{S_2\,dt}{2(S_2-t)+\sqrt{S_2(S_2-t)}}\right)\right\} \qquad (20)$$

$$D = D_1 + D_2 = \frac{\rho U_\infty^2}{2\pi}\left\{\left[\int_0^{S_1}\frac{dy_1}{dt}\frac{dt}{\sqrt{S_1-t}}\right]^2 + \left[\int_0^{S_2}\frac{dy_2}{dt}\frac{dt}{\sqrt{S_2-t}}\right]^2\right\} \qquad (21)$$

and:

$$C_L = \frac{4}{\pi}\left[\int_0^{S_1}\frac{S_1}{S_2}\frac{dy_1}{dt}\left(\frac{dt}{2(S_1-t)+\sqrt{S_1(S_1-t)}}\right) + \int_0^{S_2}\frac{dy_2}{dt}\left(\frac{dt}{2(S_2-t)+\sqrt{S_2(S_2-t)}}\right)\right] \qquad (22)$$

$$C_D = \frac{1}{\pi S_2}\left\{\left[\int_0^{S_1}\frac{dy_1}{dt}\frac{dt}{\sqrt{S_1-t}}\right]^2 + \left[\int_0^{S_2}\frac{dy_2}{dt}\frac{dt}{\sqrt{S_2-t}}\right]^2\right\} \qquad (23)$$

where the chord length in the denominator of the coefficients is s_2. By considering s_2 to be unity the expressions may be further simplified without loss of generality. Denoting the ratio between the upper and lower chord lengths $\frac{S1}{S2} = r$, we have:

$$C_L = \frac{4}{\pi}\left[\int_0^r r\frac{dy_1}{dt}\left(\frac{dt}{2(r-t)+\sqrt{r(r-t)}}\right) + \int_0^1 \frac{dy_2}{dt}\left(\frac{dt}{2(1-t)+\sqrt{1-t}}\right)\right] \tag{24}$$

$$C_D = \frac{1}{\pi}\left\{\left[\int_0^r \frac{dy_1}{dt}\frac{dt}{\sqrt{r-t}}\right]^2 + \left[\int_0^1 \frac{dy_2}{dt}\frac{dt}{\sqrt{1-t}}\right]^2\right\} \tag{25}$$

COMPARISON OF RESULTS WITH KNOWN DATA

FLAT PLATE

Since several assumptions have been made, it was considered advisable to compare the results obtained from Equations (24) and (25) with known data. The simplest comparison is that of a flat plate, where r = 0 and $\frac{dy2}{dx} = \alpha_2$. Equations (24) and (25) thus become:

$$C_L = \frac{4}{\pi}\alpha_2\int_0^1 \frac{dt}{2(1-t)+\sqrt{1-t}} = \frac{4}{\pi}\alpha_2 \ln 3 \cong 1.40\alpha_2 \tag{26}$$

$$C_D = \frac{1}{\pi}\alpha_2^2\left[\int_0^1 \frac{dt}{\sqrt{1-t}}\right]^2 = \frac{4}{\pi}\alpha_2^2 \cong 1.27\alpha_2^2 \tag{27}$$

The coefficients from exact theory[8] are:

$$C_L = \frac{2\pi\sin\alpha_2\cos\alpha_2}{4+\pi\sin\alpha_2} = \frac{\pi\alpha_2}{2} + O(\alpha_2^2) \cong 1.57\alpha_2 \tag{28}$$

$$C_D = C_L\tan\alpha_2 = \frac{\pi\alpha_2^2}{2} + O(\alpha_2^3) \cong 1.57\alpha_2^2 \tag{29}$$

Thus for the case of a flat plate, the approximate solution for the lift coefficient is seen to be low by about 12% and the solution for the drag coefficient is low by about 23%. Actually the smaller error in the case of lift is due only to the series approximation, Equation (18e), which raises the lift coefficient in the case of the flat plate by the

ratio $\ln 3$ to 1, or about 10%. Applying Equation (18d) to the flat plate gives:

$$C_L = \frac{4}{\pi}\alpha_2 \cong 1.27\alpha_2 \tag{27a}$$

Another exact theory which is known and is more pertinent to the foils being considered is that for a non-symmetrical wedge (Figure 2). For this case the exact theory[7] gives:*

$$C_D = \frac{2a^2(\alpha_2-\alpha_1)^2}{U_\infty \pi S_2}\cos^2\frac{\pi}{2}\left(\frac{\alpha_1+\alpha_2}{\alpha_1-\alpha_2}\right) \tag{30}$$

$$C_L = \frac{a^2}{U_\infty S_2}(\alpha_2-\alpha_1)\sin\pi\left(\frac{\alpha_1+\alpha_2}{\alpha_1-\alpha_2}\right) \tag{31}$$

the constant a is determined from the integral equation:

$$a^2 = \frac{U_\infty S_2}{2\int_0^\omega e^{-\tau}(\cos\chi-\cos\omega)\sin\chi\, d\chi}$$

where: $\omega = \frac{\pi\alpha_1}{\alpha_1-\alpha_2}$

and: $\tau = \left(\frac{\alpha_2-\alpha_1}{2\pi}\right)\ln\left(\frac{\sin^2\frac{1}{2}(\chi-\omega)}{\sin^2\frac{1}{2}(\chi+\omega)}\right)$

For a thin wedge ($\alpha_2-\alpha_1 \ll \pi$) Equations (30) and (31) become (Appendix C):

$$C_D = \frac{2}{\pi}\frac{\alpha_2-\alpha_1}{1-\cos\omega}\cos\frac{\pi}{2}\left(\frac{\alpha_1+\alpha_2}{\alpha_1-\alpha_2}\right)^2 \tag{30a}$$

$$C_L = \frac{\alpha_2-\alpha_1}{(1-\cos\omega)^2}\sin\pi\left(\frac{\alpha_1+\alpha_2}{\alpha_1-\alpha_2}\right) \tag{31a}$$

---

* Note that the sign of α_1 has been changed from that in Milne-Thomson to conform with the convention of this paper. Thus α_1 as shown in Figure 2 has a negative value.

This solution also is based on the condition that the stagnation point is at the leading edge, and the condition for this is that the ratio of chord lengths be:

$$r = \frac{s_1}{s_2} = \frac{\int_{\pi}^{\omega} e^{-\tau}(\cos\chi - \cos\omega)\sin\chi\, d\chi}{\int_{0}^{\omega} e^{-\tau}(\cos\chi - \cos\omega)\sin\chi\, d\chi} \cong \left(\frac{1+\cos\omega}{1-\cos\omega}\right)^2 \qquad (32)$$

Using Equation (32), the approximate solution (Equations 24 and 25) gives the following results:

$$C_L = \frac{4}{\pi}\left(r\frac{dy_1}{dt} + \frac{dy_2}{dt}\right)\ln 3 = \frac{4}{\pi}\left(r\alpha_1 + \alpha_2\right)\ln 3 \qquad (33)$$

$$C_D = \frac{4}{\pi}\left(r\alpha_1^2 + \alpha_2^2\right) \qquad (34)$$

For the purpose of comparing the exact and approximate solutions, values of $\frac{C_L}{\alpha_2}$, $\frac{C_D}{\alpha_2^2}$, and $-\frac{\alpha_2}{\alpha_1}$ have been plotted vs. r (Figure 4). As was the case with the flat plate, the approximate solutions for both lift and drag are somewhat lower than the exact solutions. Both coefficients approach the exact solutions as r approaches unity, or a symmetrical wedge.

A third comparison has been made with experimental data for a circular arc section,[9] Figure 3. The experimental data (Figure 5) is shown in a plot of lift and drag coefficients vs. cavitation number for 8 degrees angle of attack. At this angle separation did not occur at the leading edge, but instead at the discontinuity of the upper surface. Thus the flow corresponds exactly to that of Figure 1. The experimental points are marked as circles on the graph, and the solid lines represent the predicted coefficients assuming full cavitation from the leading edge according to Wu's theory[2].

Applying the approximate solutions to the circular arc at 8 degrees angle of attack and zero cavitation number gives the following results (Appendix D):

	C_L	C_D
Separation at Leading Edge	0.298	0.0457
Separation at the Bend	0.165	0.0691

These points have been plotted on the $\sigma = 0$ ordinate of Figure 5. Again the lift coefficient is low, by about 13% when separation occurs at the leading edge. Unfortunately, experimental data is not available below $\sigma = 0.2$, but the general trend of the points seems to be close to that given by $C_{L_1} + C_{L_2}$. The approximate solution gives a drag coefficient which is about 10% high for the case of cavitation from the leading edge and the general trend of the experimental points is in the direction of $C_{D_1} + C_{D_2}$.

DISCUSSION OF THE RESULTS

In the development of the solution it has been assumed that the stagnation streamline was horizontal, thus allowing the face and back to be treated separately, and that the lift and drag forces due to the velocities induced by the body source distribution were zero. As a result this solution is only an approximate one, the accuracy of which can only be determined from comparison with known data, such as is done in the preceding section. The greatest divergence from known data is in the case of the flat plate, where the approximate solution for drag is 23% less than the exact solution. Strictly speaking this comparison should not be made since the stagnation point is not at the leading edge, unless $\alpha_2 = 0$, in which case the comparison becomes trivial. The difference between the two solutions should not be taken lightly since it is not known to what extent the position of the stagnation point will influence the final accuracy. If no other conclusion can be drawn from this, it can at least be seen that it is possible for a solution based on completely different conditions to give an answer which is approximately correct.

Comparisons with data for foils where the stagnation point is at the leading edge are more encouraging. For the case of the non-symmetrical wedge, or equivalently the foil with flat surfaces, the lift and drag coefficients are both low, but for $r \geq .05$, the maximum difference is only about 7% for both, and as r increases the difference becomes smaller. There is no assurance, of course, that the same accuracy will exist for a foil with curved surfaces, and this fact is borne out by the comparison with experimental data, although this latter comparison is a rather indefinite one.

In any event, the accuracy of the results is sufficient for the conclusion to be drawn that the performance of a foil with a partially wetted back is greatly inferior to a fully cavitating foil. This is shown for the wedge in Figure 6 where $\frac{L\alpha_2}{D}$ is plotted vs. r. In this case when the back is wetted over 5% of the chord length, there will be a loss in lift-drag ratio of 30% as compared to a fully cavitating flat plate. The obvious conclusion to be drawn therefore, is that a partially wetted back should be avoided if at all possible.

RECOMMENDATIONS

There are two principal shortcomings in the solution as it now stands. The first is that assumptions have been made which diminish the accuracy and thus the authority of the results. The second is that the assumption is made that the stagnation point is at the leading edge without stating the conditions under which this will be so.

The approximating assumptions can best be overcome by solving the problem by conformal mapping. This has been attempted without success but further efforts would be worthwhile.

Determining the conditions at which the stagnation point will be at the leading edge, or particularly, the angle of attack for any given foil, would also contribute greatly to the value of the solution. Milne-Thomson solved this problem for the non-symmetrical wedge (Equation 32), but no solution has been obtained for curved surfaces.

Further research could also be directed toward extending the solution to cover finite cavitation numbers. It is quite possible that the effect of the partially-wetted back is not as great under such conditions, and this information would be most valuable for design purposes.

ACKNOWLEDGEMENTS

The author is indebted to A. J. Tachmindji for his constant help and encouragement throughout the investigation.

REFERENCES

1. Tulin, M. P., "Supercavitating Flow Past Foils and Struts," Proceedings of a Symposium on Cavitation in Hydrodynamics, National Physical Laboratory, September 1955, H. M. Stationery Office

2. Wu, T. Yao-tsu, "A Free Streamline Theory for Two-Dimensional Fully Cavitated Hydrofoils," Report No. 21-17, Hydrodynamics Laboratory, CIT, Pasadena, California, July 1955.

3. Tulin, M. P., "Steady Two-Dimensional Cavity Flows About Slender Bodies," TMB Report 834, May 1953

4. Birkhoff, G., "Hydrodynamics," Princeton University Press for University of Cincinnati, 1950.

5. Gilbarg, D. and Rock, D. H., "On Two Theories of Plane Potential Flows with Finite Cavities," Naval Ordnance Lab. Memorandum 8718, August 1946.

6. Cheng, H. K. and Rott, N., "Generalization of the Inversion Formula of Thin Airfoil Theory," Journal of Rational Mechanics and Analysis, Vol. 3, No. 3, 1954

7. Milne-Thomson, L. M., "Theoretical Hydrodynamics," The McMillan Company, New York, 1938, 1950.

8. Lamb. H., "Hydrodynamics," Sixth Edition, Dover Publications, New York, 1945.

9. Parkin, B. R., "Experiments on Circular Arc and Flat Plate Hydrofoils in Noncavitating and in Full Cavity Flow," Report No. 47-6, CIT, Hydrodynamics Laboratory, Pasadena, California, February 1956.

APPENDIX A

SOLUTION OF FREQUENTLY USED INTEGRALS

Let $I(m, n, \varphi, \psi) = \int_{\psi}^{\varphi} \sqrt{\frac{z}{m-z}} \frac{dz}{(z-n)}$

Substituting $z = m\sin^2\theta$ gives:

$$I(m,n,\varphi,\psi) = 2\int_{\sin^{-1}\sqrt{\frac{\psi}{m}}}^{\sin^{-1}\sqrt{\frac{\varphi}{m}}} \frac{\sin^2\theta\, d\theta}{-\cos^2\theta + 1 - n/m} = -2\sqrt{\frac{n/m}{1-n/m}} \tan^{-1}\left(\sqrt{\frac{1-n/m}{-n/m}} \tan\theta\right) + 2\theta \Bigg]_{\sin^{-1}\sqrt{\frac{\psi}{m}}}^{\sin^{-1}\sqrt{\frac{\varphi}{m}}}$$

$$I(m,n,\varphi,\psi) = 2\left[\sin^{-1}\sqrt{\varphi/m} - \sin^{-1}\sqrt{\psi/m} - \sqrt{\frac{n}{n-m}}\left(\tan^{-1}\sqrt{\frac{\varphi(n-m)}{n(m-\varphi)}} - \tan^{-1}\sqrt{\frac{\psi(n-m)}{n(m-\psi)}}\right)\right]$$

for the solution of $\int_s^{\ell} \sqrt{\frac{\ell-x'}{x'-s}} \frac{dx'}{x'-x} = Re\left[I(\ell-s, \ell-x, 0, \ell-s)\right]$

$$\int_s^{\ell} \sqrt{\frac{\ell-x'}{x'-s}} \frac{dx'}{x'-x} = \begin{cases} -\pi & \text{for} \quad \ell > x > s \\ -\pi\left(1-\sqrt{\frac{\ell-x}{s-x}}\right) & \text{for} \quad \ell > x,\ s > x \end{cases}$$

and for the solution of $\int_s^{\ell} \sqrt{\frac{\ell-x'}{x'-s}} \frac{dx'}{(x'-x)(x'-t)}$

$$= Re\left\{\frac{1}{t-x}\left[I(\ell-s, \ell-x, 0, \ell-s) - I(\ell-s, \ell-t, 0, \ell-s)\right]\right\}$$

$$= \frac{\pi}{t-x}\sqrt{\frac{t-\ell}{t-s}} \qquad \text{for} \quad \ell > x > s > t > 0$$

APPENDIX B

EVALUATION OF THE SECOND INTEGRAL OF EQUATION (15)

$$\int_0^s \frac{dy_0}{dt} \int_s^\ell \sqrt{\frac{x'-s}{\ell-x'}}\, \frac{1}{t-x'} \int_0^s \frac{dy_0}{d\tau} \sqrt{\frac{\tau-\ell}{\tau-s}}\, \frac{d\tau}{x'-\tau}\, dx'\, dt$$

$$= \int_0^s \frac{dy_0}{dt} \int_0^s \frac{dy_0}{d\tau} \sqrt{\frac{\tau-\ell}{\tau-s}} \int_s^\ell \sqrt{\frac{x'-s}{\ell-x'}}\, \frac{dx'}{(t-x')(x'-\tau)}\, d\tau\, dt$$

$$= \int_0^s \frac{dy_0}{dt} \int_0^s \frac{dy_0}{d\tau} \sqrt{\frac{\tau-\ell}{\tau-s}} \left\{ Re\, \frac{1}{t-\tau} \left[I(\ell-s, \tau-s, \ell-s, 0) - I(\ell-s, t-s, \ell-s, 0) \right] \right\}$$

$$= \int_0^s \frac{dy_0}{dt} \int_0^s \frac{dy_0}{d\tau} \sqrt{\frac{\tau-\ell}{\tau-s}} \left\{ \frac{\pi}{t-\tau} \left[\sqrt{\frac{t-s}{t-\ell}} - \sqrt{\frac{\tau-s}{\tau-\ell}} \right] \right\} d\tau\, dt$$

$$= \int_0^s \frac{dy_0}{dt} \int_0^s \frac{dy_0}{d\tau} \frac{\pi}{t-\tau} \sqrt{\left(\frac{\tau-\ell}{\tau-s}\right)\left(\frac{t-s}{t-\ell}\right)}\, d\tau\, dt - \int_0^s \frac{dy_0}{dt} \int_0^s \frac{dy_0}{d\tau} \frac{\pi}{t-\tau}\, d\tau\, dt$$

but: $$\int_0^s \frac{dy_0}{dt} \int_0^s \frac{dy_0}{d\tau} \frac{d\tau}{t-\tau} = \int_0^s \frac{dy_0}{dt} \int_0^s \frac{m(\tau)}{2U_c} \frac{dt}{t-\tau} = \frac{2}{U_c} \int_0^s \frac{dy_0}{dt}\, u_{0\text{-}0}(t) = 0$$

therefore: $$\int_0^s \frac{dy_0}{dt} \int_s^\ell \sqrt{\frac{x'-s}{\ell-x'}}\, \frac{1}{t-x'} \int_0^s \frac{dy_0}{d\tau} \sqrt{\frac{\tau-\ell}{\tau-s}}\, \frac{d\tau}{x'-\tau}\, dx'\, dt = J$$

where: $$J = \pi \int_0^s \int_0^s \frac{dy_0}{dt} \frac{dy_0}{d\tau} \sqrt{\left(\frac{\tau-\ell}{\tau-s}\right)\left(\frac{t-s}{t-\ell}\right)}\, \frac{d\tau\, dt}{t-\tau}$$

J is determined as follows:

$$J = \pi \int_0^S \int_0^S \frac{dy_0}{dt}\,\frac{dy_0}{d\tau}\sqrt{\left(\frac{t-\ell}{t-s}\right)\left(\frac{\tau-s}{\tau-\ell}\right)}\,\frac{dt\,d\tau}{\tau-t} = -\pi \int_0^S \int_0^S \frac{dy_0}{d\tau}\,\frac{dy_0}{dt}\sqrt{\left(\frac{\tau-\ell}{\tau-s}\right)\left(\frac{t-s}{t-\ell}\right)}\,\frac{d\tau\,dt}{\tau-t}$$

$$= \frac{\pi}{2} \int_0^S \int_0^S \frac{dy_0}{dt}\,\frac{dy_0}{d\tau}\left[\sqrt{\left(\frac{\tau-\ell}{\tau-s}\right)\left(\frac{t-s}{t-\ell}\right)} - \sqrt{\left(\frac{t-\ell}{t-s}\right)\left(\frac{\tau-s}{\tau-\ell}\right)}\right]\frac{dt\,d\tau}{t-\tau}$$

$$= \frac{\pi}{2} \int_0^S \int_0^S \frac{dy_0}{dt}\,\frac{dy_0}{d\tau}\left[\frac{(\tau-\ell)(t-s)-(t-\ell)(\tau-s)}{\sqrt{(\tau-s)(\tau-\ell)(t-s)(t-\ell)}}\right]\frac{dt\,d\tau}{t-\tau}$$

$$= \pi\,\frac{s-\ell}{2} \int_0^S \int_0^S \frac{dy_0}{dt}\,\frac{dy_0}{d\tau}\,\frac{dt\,d\tau}{\sqrt{(\tau-s)(\tau-\ell)(t-s)(t-\ell)}}$$

$$J = \pi\,\frac{s-\ell}{2}\left[\int_0^S \frac{dy_0}{dt}\,\frac{dt}{\sqrt{(t-s)(t-\ell)}}\right]^2$$

APPENDIX C

SOLUTION OF EQUATIONS (30), (31), and (32)

since: $$e^{-\left(\frac{\alpha_2-\alpha_1}{2\pi}\right)\ln\left(\frac{\sin \frac{1}{2}(\chi-\omega)}{\sin \frac{1}{2}(\chi+\omega)}\right)^2} = \left(\frac{\sin \frac{1}{2}(\chi-\omega)}{\sin \frac{1}{2}(\chi+\omega)}\right)^{-\frac{\alpha_2-\alpha_1}{\pi}}$$

and: $$\cos\chi - \cos\omega = -2\sin\tfrac{1}{2}(\chi+\omega)\sin\tfrac{1}{2}(\chi-\omega)$$

then: $$\int_0^{\omega} e^{-\tau}(\cos\chi-\cos\omega)\sin\chi\,d\chi$$

$$= -2\int_0^{\omega}\left[\sin\tfrac{1}{2}(\chi+\omega)\right]^{1+\frac{\alpha_2-\alpha_1}{\pi}}\left[\sin\tfrac{1}{2}(\chi-\omega)\right]^{1-\frac{\alpha_2-\alpha_1}{\pi}}\sin\chi\,d\chi$$

Assuming a thin wedge, $\frac{\alpha_2-\alpha_1}{\pi} \ll 1$, and the integral may be approximated by:

$$-2\int_0^{\omega}\sin\tfrac{1}{2}(\chi+\omega)\sin\tfrac{1}{2}(\chi-\omega)\sin\chi\,d\chi$$

$$= \int_0^{\omega}(\cos\chi-\cos\omega)\sin\chi\,d\chi = \tfrac{1}{2}(1-\cos\omega)^2$$

and by the same method:

$$\int_{\pi}^{\omega} e^{-\tau}(\cos\chi-\cos\omega)\sin\chi\,d\chi = \tfrac{1}{2}(1+\cos\omega)^2$$

Thus: $$a^2 = \frac{US_2}{(1-\cos\omega)^2}$$

and: $$\frac{S_1}{S_2} = \left(\frac{1+\cos\omega}{1-\cos\omega}\right)^2$$

APPENDIX D

CALCULATION OF LIFT AND DRAG COEFFICIENTS FOR THE CIRCULAR ARC SECTION

At 8° angle of attack, the face is tangent to the x-axis at the leading edge:

$$\frac{dy_2}{dx}(0) = 0$$

Therefore, since the face is a circular arc of radius R:

$$\frac{dy_2}{dx} = \tan\theta \quad \text{where } \theta = \sin^{-1}\frac{x}{R}$$

$$\frac{dy_2}{dx} = \tan\left(\sin^{-1}\frac{x}{R}\right) = \frac{x}{\sqrt{R^2-x^2}}$$

And:
$$\frac{dy_1}{dx} = \alpha_1 = \tan\left(8^\circ - \tan^{-1}\frac{0.400}{1.162}\right) = -0.194$$

Also, for equations (24) and (25) to hold, s_2 must be unity which determines R:

$$R = \frac{8.55}{2.38} = 3.59$$

and:
$$r = \frac{s_1}{s_2} = \frac{1.162}{2.380} = 0.488$$

Equations (24) and (25) become:

$$C_L = \frac{4}{\pi}\int_0^r r\alpha_1 \frac{dx}{2(r-x)+\sqrt{r(r-x)}} + \int_0^1 \frac{x}{\sqrt{R^2-x^2}} \frac{dx}{2(1-x)+\sqrt{1-x}} \tag{24a}$$

$$C_D = \frac{1}{\pi}\left\{\left[\int_0^r \alpha_1 \frac{dx}{\sqrt{r-x}}\right]^2 + \left[\int_0^1 \frac{x\,dx}{\sqrt{R^2-x^2}\sqrt{1-x}}\right]^2\right\} \tag{25a}$$

The first integral in each equation is easily evaluated to give C_{L_1} and C_{D_1}:

$$C_{L_1} = -\frac{4}{\pi} r\alpha_1 \ln 3 = -0.133$$

$$C_{D_1} = \frac{1}{\pi}\left(-2\alpha_1\sqrt{r}\right)^2 = +0.0234$$

But the evaluation of the integrals for C_{L_2} and C_{D_2} is considerably more difficult. Consequently, they were simplified by assuming $\sqrt{R^2-x^2}$ = constant. Since the maximum value is R = 3.59 and the minimum value is $\sqrt{R^2-1}$ = 3.45, the error involved is small.

The average value was taken as 3.52.

Thus:

$$C_{L_2} = \frac{4}{3.52\pi}\int_0^1 \frac{x\,dx}{2(1-x)+\sqrt{1-x}} = 0.298$$

$$C_{D_2} = \frac{11}{7\pi}\left[\frac{16}{3.52}\int_0^1 \frac{x\,dx}{\sqrt{1-x}}\right]^2 = 0.0457$$

Thus:

$$C_L = 0.298 - 0.133 = 0.165$$

$$C_D = 0.0457 + 0.0234 = 0.0691$$

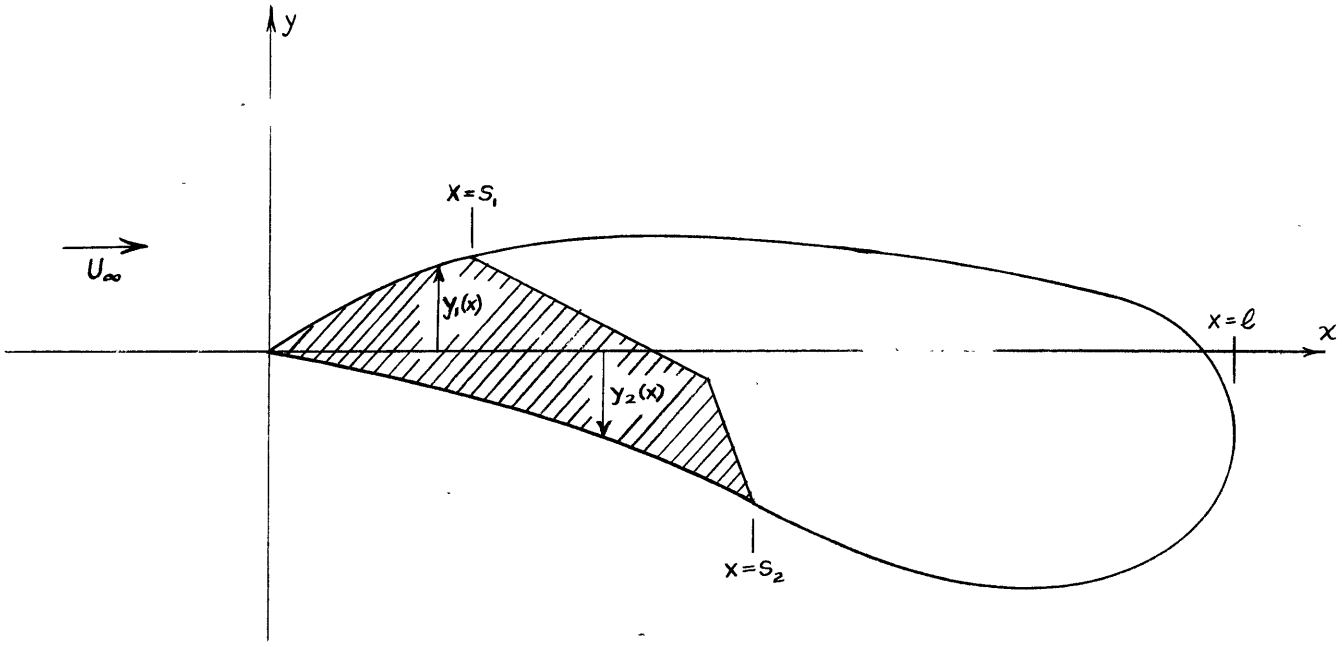

Figure 1 - Diagram of the Foil in Super-Cavitating Flow

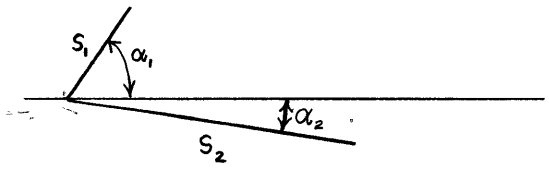

Figure 2 - The Foil as a Non-Symmetrical Wedge

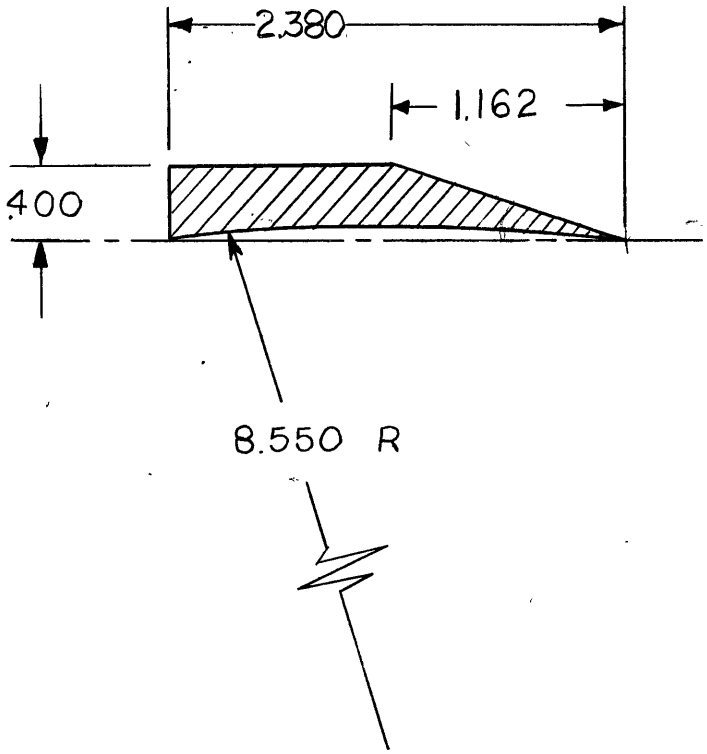

Figure 3 - The Circular Arc Section

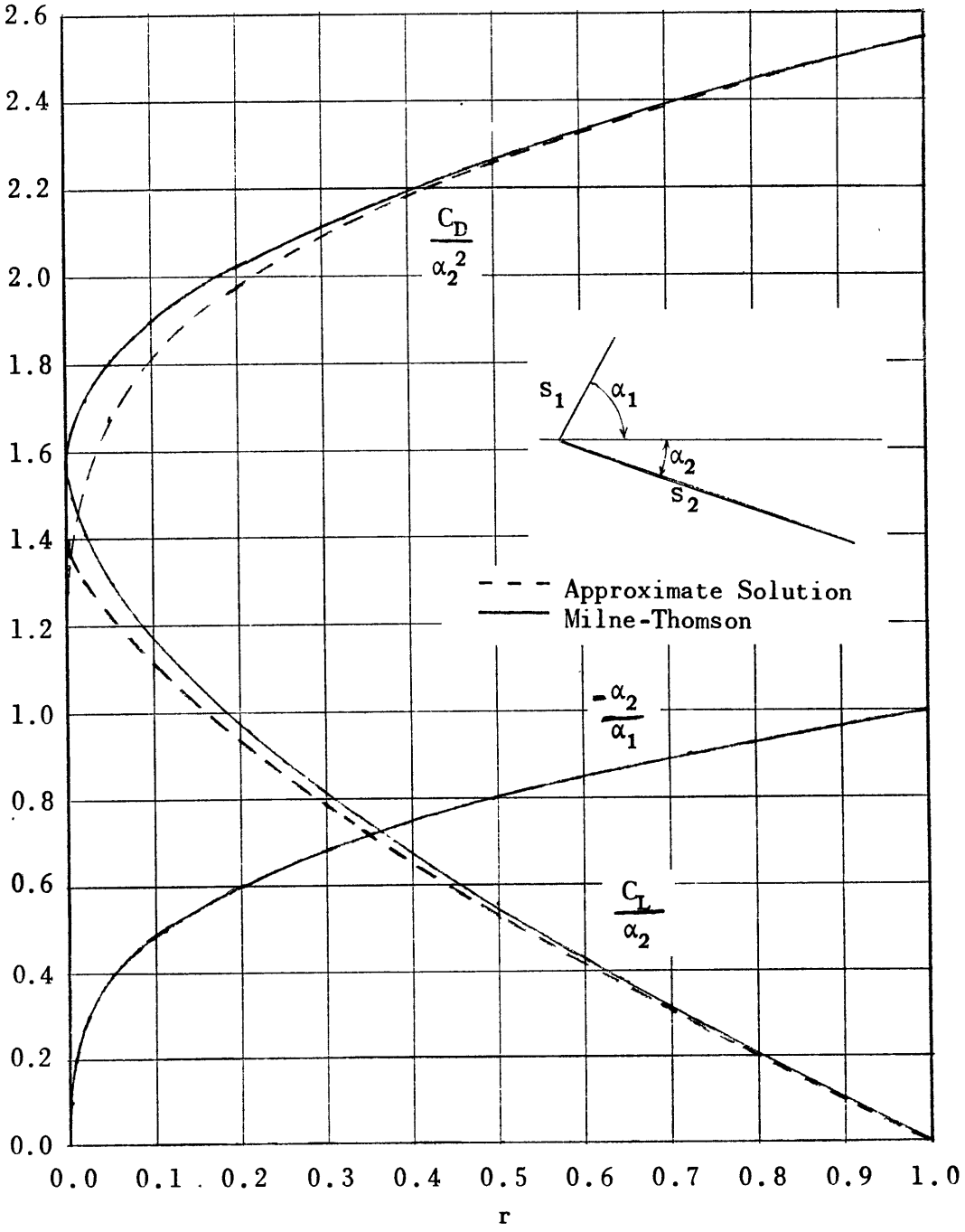

Figure 4 - Lift and Drag Coefficients for Thin Non-Symmetrical Wedges

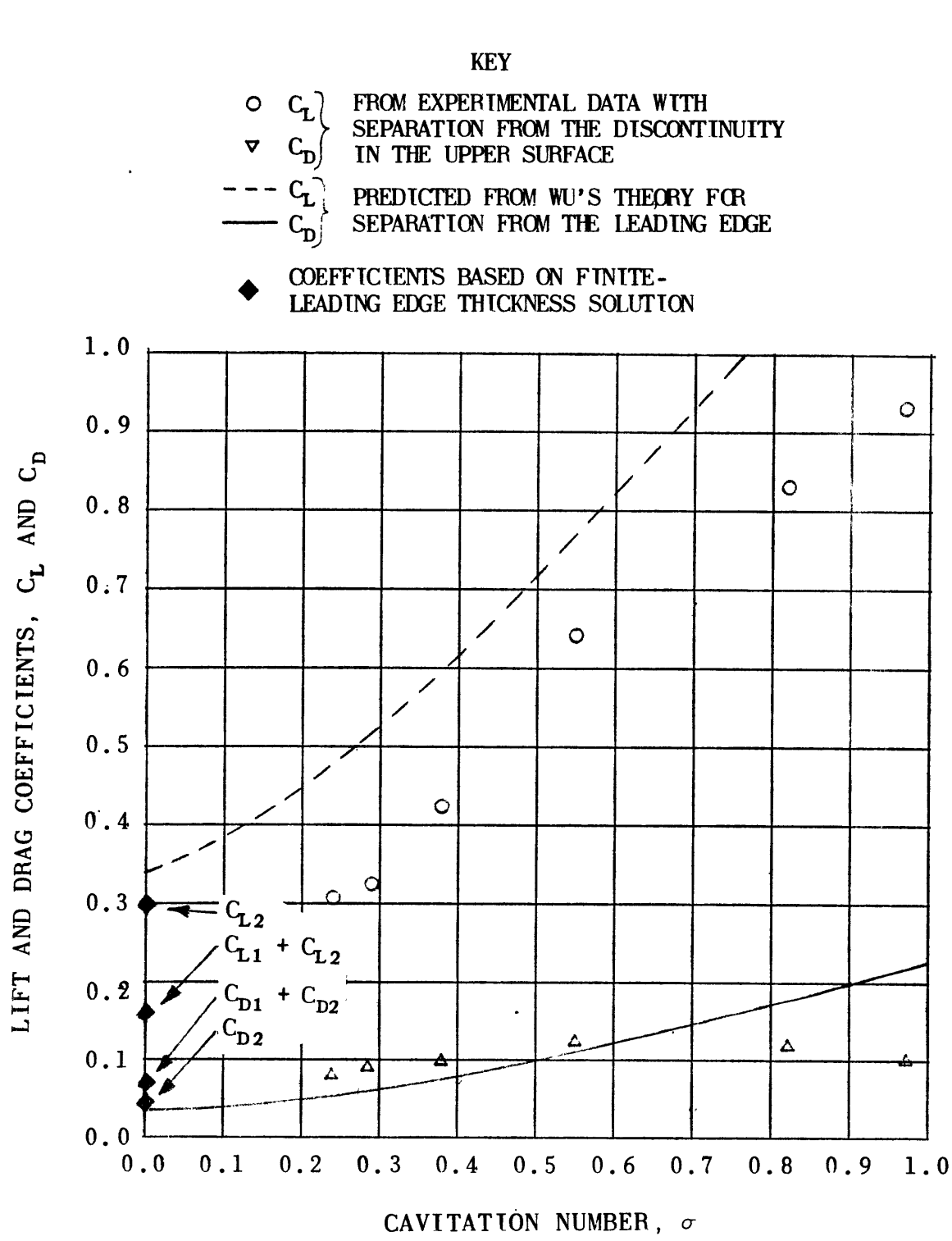

Figure 5 - Comparison of Approximate Solution with Experimental Data for Circular Arc Section at 8° Angle of Attack

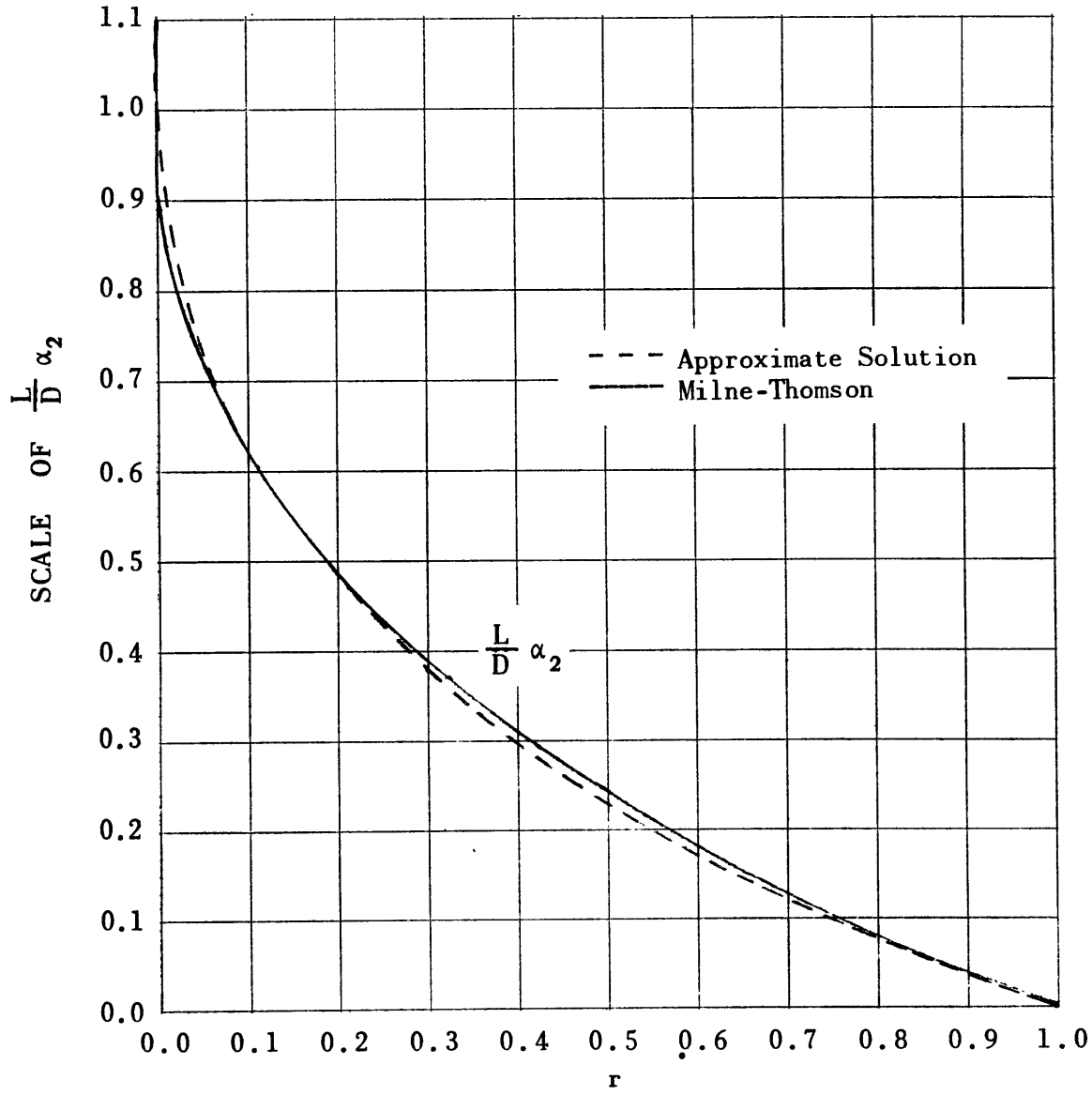

Figure 6 - Lift-Drag Ratios For Thin Non-Symmetrical Wedges

INITIAL DISTRIBUTION

Copies	
8	Chief, Bureau of Ships, Technical Library (Code 312), for distribution: 5 - Technical Library 1 - Civilian Consultant to the Chief (Code 106) 1 - Preliminary Design (Code 421) 1 - Propeller and Shafting (Code 554)
2	Chief of Naval Research, Fluid Mechanics Branch, Code 438, Attn: M. L. Tulin
1	Director, Ordnance Research Lab., Penn State University, University Park, Pa.
1	Commander, Naval Ordnance Test Station, Pasadena Annex, Pasadena, California
1	Experimental Towing Tank, Stevens Institute of Technology, 711 Hudson Street, Hoboken, N.J.
1	Head, Department of Naval Architecture and Marine Engineering, MIT, Cambridge 39, Mass., Attn: Prof. L. Troost
1	Director, National Advisory Committee for Aeronautics, Langley Field, Va., Attn: Mr. Parkinson
1	Director, National Advisory Committee for Aeronautics, Washington, D. C.
1	Gibbs & Cox, Inc., 21 West St., New York 6, N. Y., Attn: Dr. S. F. Hoerner
1	Director, Iowa Institute of Hydraulic Research, State University of Iowa, Iowa City, Iowa
1	Director, St. Anthony Falls Hydraulic Lab., University of Minnesota, Minneapolis 14, Minn.
1	Director, Hydrodynamic Lab., California Institute of Technology, Pasadena 4, Calif.
9	British Joint Services Mission (Navy Staff), P. O. Box 165, Benjamin Franklin Station, Washington, D. C.
3	Canadian Joint Staff, 1700 Mass. Ave., N.W. Washington 6, D. C.